

Microstructural aging of bitumen

Daniel Großegger

physical chemistry, institute of material chemistry, Vienna, Austria

groszegger.daniel@gmail.com

Digital Object Identifier (DOI): dx.doi.org/10.14311/EE.2016.135

ABSTRACT

The microstructure of bitumen undergoes alteration over time, referred to as ageing. These structural changes affect the behaviour of bitumen, which can be verified by conventional or performance orientated testing methods. With different imaging techniques, like confocal laser scanning microscopy, atomic force microscopy and transmission electron microscopy, these changes can be made visible. An important issue regards the used methods for acquiring aged bitumen. Hence field aged bitumen (reclaimed from asphalt) and artificial aged bitumen (produced by RTFOT and PAV) are investigated. It seems as if a correlation between the size of microcapsule (often referred to as micelle) and the age of bitumen exists. By separating bitumen into 4 fractions (saturates, aromatics, resins and asphaltenes) the respective percentage are determined and an attempt of allocating the fractions to the visualised microstructure will be done.

Keywords: Ageing

1. INTRODUCTION

As a demand orientated residue of petroleum refinery, bitumen consist mainly of hydrocarbons of different molecular sizes and contains additionally small amounts of heteroatoms like oxygen, nitrogen, sulphur and traces of metals. A practicable method for separating this complex mixture into generic fractions is due to their different solubilities and polarities. A common approach is the SARA (Saturates-Aromatics-Resins-Asphaltenes) analysis. Asphaltenes are defined by their insolubility in aliphatic solvents, but soluble in aromatic solvents. Maltenes, as aliphatic soluble part, are further separated by chromatographic column separation – based on polarity – into saturates, aromatics and resins [1, 2].

Modern analytical visualization techniques revealed, that there are structuring features within bitumen. Different techniques observed different properties of these features. Atomic force microscopy and scanning electron microscopy uncovered surface structures of 1-5 μm sizes, often referred to as “bee-like” structures or catana phase [3-10]. Confocal laser scanning microscopy discovered fluorescent centres with a size of 1-10 μm [11-13]. Despite many publications on bitumen microstructures, it is still unknown if these features are linked and if these observed surface structures are based on bulk structures or not. Further, the identification and allocation of bitumen fractions toward the structure is not consistent. The origin of the fluorescence centres could be caused by asphaltenes [11], wax content [12] or aromatics [13]. The structure observed by atomic force microscopy was linked with asphaltene content, wax crystallization or metal content of the bitumen [5,6,9,10]. Simulations suggested that the interaction of all fractions is the reason behind the different appearance of the structures [14].

2. MATERIALS AND METHODS

2.1. Bitumen and separation

The bitumen used was an unmodified 70/100 pen with a penetration of 91 1/10 mm. For ageing standard laboratory ageing methods were used. Therefore bitumen was first treated by rolling thin film oven test [15], followed by pressure ageing vessel (PAV) [16], which simulates about 5 years of road service life. Additionally an unmodified bitumen extracted from an field core sample was investigated by AFM, which had originally a penetration of 83 1/10 mm and after a service lifetime of 23,5 years the value decreased to 27 1/10 mm. Properties of the bitumen used are given in Table 1.

The separation into four fractions was done according to a modified ASTM standard 4124-01 [17]. Around 11 g to 12,5 g of bitumen were weighted into a round bottom flask and about 500 ml of *n*-heptane were added. The dispersion was heated until the boiling point was reached and kept at this temperature for at least one hour. Thereafter the flask was set aside overnight to allow the insoluble particle, mostly asphaltenes, to sediment. The next day the dispersion was washed through a filter with particle retention of 2 μm (obtained from VWR International). The filter with the filter cake was folded and placed inside a Soxhlet extractor [18] to remove further *n*-heptane soluble parts adhering to the asphaltenes. After about 3 days the solution from the Soxhlet extraction process was filtered again to verify the absence of asphaltenes. The solution was then concentrated and placed on the top of a 450 g dense packed aluminium oxide column pretreated with *n*-heptane. The eluents used were *n*-heptane (200 ml), methylbenzene (400 ml), an equal mixture of methanol and methylbenzene (300 ml) and trichloroethene (500 ml). The cut points between the fractions were chosen by visual colour change. The excess solvent of the three fractions obtained by liquid column chromatography was removed by a rotary evaporator at 160 °C and 10 mbar. The powder like asphaltenes were desiccated in an oven at 120 °C. The solvents *n*-heptane, methylbenzene, methanol had at least a purity of 99% or higher and the purity of trichloroethene was 98% or higher. All chemicals used were obtained from Carl Roth.

2.2. Confocal laser scanning microscopy (CLSM)

For sample preparation bitumen was heated to a temperature between 150 °C and 200 °C. Three small droplets were placed on a precision coverslip (< 0,2 mm), situated on a 150 °C heated heating plate. A second coverslip was placed on top of the droplets and slight force was applied to receive a thin bitumen film between the precision coverslips. The samples were measured within 4 to 6 hours after preparation. The sample storage took place at room temperature.

The confocal laser scanning microscope used was an ECLIPSE TE2000 with a transmission and a CLSM array. The light source for transmission was a T-DH 100W Illumination Pillar and for the excitation radiation an argon-ion laser was used at an excitation wavelength of 488 nm. A band pass filter 515/30 was equipped for detection, providing an observation window between 500 nm and 530 nm.

2.3. Cryo-transmission electron microscopy (cryo-TEM)

Only the unaged bitumen was investigated with this technique. The bitumen was heated on a heating plate to the range of about 120 °C to 150 °C, to be less viscous. Then the tip of an aluminium bar, with dimension of about 10 mm length and 3 mm in diameter, was dipped into the heated bitumen, to obtain a droplet of bitumen covering the tip of the bar. After cooling down to room temperature and a rest period of 24 hours, the bar with the droplet entered the RMC cryo-microtome and was cooled down with liquid nitrogen to a temperature of approximately -20 °C to -30 °C. The now

brittle sample was cut with a diamond knife in flakes of about 100 nm thicknesses. These flakes were deposited onto a sample holder for the cryo-TEM. Until placed on a double tilt cryo-transfer sample holder, the sample was stored in liquid nitrogen. The sample holder was inserted into the cryo-TEM, which was a FEI TECNAI G20 – low voltage setup with a lattice resolution of 0,14 nm. After ultra-high vacuum was reached the recoding of the images started. All steps were carried out without thawing by cooling the sample with liquid nitrogen.

2.4. Atomic force microscopy (AFM)

A bitumen drop was placed on a round steel plate with a diameter of approximately 10 mm and then smeared to cover a larger part of the plate. This was done for unaged and aged bitumen, as well as for the recovered bitumen. In order to obtain an even bitumen surface, the samples were placed for approximately 30 minutes inside an 120 °C hot oven. To allow the formation of the typical surface features the samples were stored at ambient temperatures for a minimum of 24 hours.

The AFM force mapping was performed with a NanoScope V from Bruker in PeakForce QNM (Quantitative Nanomechanical property Mapping). The force-distance-curve was obtained at a resonance frequency of 3 kHz. The tip used was not calibrated and hence the topography overlay with elastic modulus is used only for comparison within the samples.

3. RESULTS AND DISCUSSION

Ageing causes a change in the distribution of fractions (Table 1) by fragmentation, polymerisation and uptake of oxygen [19,20]. The saturate content is not altered during laboratory ageing, due to their lesser reactivity towards oxygen [19]. In field samples a minor amount can evaporate or react with atmospheric radicals, which could explain the loss in saturates for the field obtained sample. They become more polar and less soluble in alkanes by oxygen uptake into their molecular structure. Hence the aromatic content decreases and the asphaltene content increases during ageing. The amount of resins depends on the ageing time; a slow shift from aromatics to resins and further to asphaltenes.

Table 1: Bitumen properties

	70/100 unaged	70/100 aged	field sample aged
penetration, 1/10 mm	91	30	27
softening point, °C	46,2	58,4	58,8
asphaltenes, wt%	9,9	14,8	19,4
saturates, wt%	8,7	8,7	8,5
aromatics, wt%	48,1	38,7	36,9
resins, wt%	32,9	37,1	35,2
colloidal instability index	0,23	0,31	0,39

Small fluorescing regions in the size of about 1 µm to 2 µm appear in both – unaged and aged – bitumen and are evenly distributed (Figure 1). Microscope images in transmission mode (Figure 1, right) revealed additional features, but these seemed to be by some means correlated with the fluorescing regions. Fluorescence centres can be found at the same location where smaller darker or brighter spots appeared. They appear a bit larger than the spots in the microscope image. Similar features were found for these samples with reflected-light microscope on the surfaces.

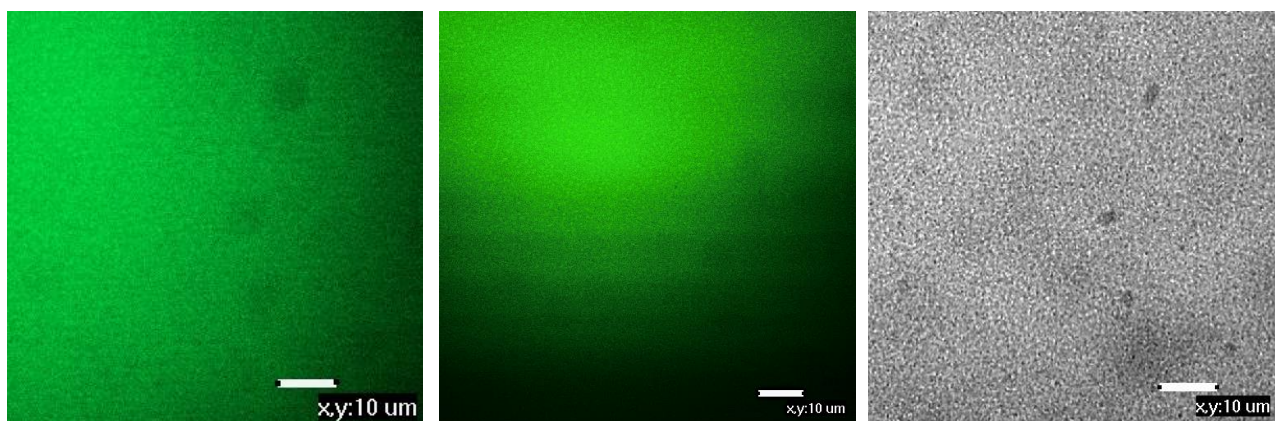


Figure 1: Confocal laser scanning images of 70/100 unaged (left), 70/100 aged (middle) and microscope image of 70/100 aged (right)

The bitumen investigated showed the three phases observable by AFM: the corrugated catana phase (“bee-structures”), the encapsulating phase around it, called peri-phase, embedded in the para-phase [4]. The elliptical catana phase and the peri-phase increase in size from unaged to aged bitumen (Figure 2). The geometrical features of the catana phase for unaged bitumen are approximately 3,6 μm (major axis) and 0,5 μm (minor axis). The minor axis of the peri-phase is about 2,7 μm . For aged bitumen the major axis increases to 7,3 μm . The field aged sample does not feature the same structure as unaged and aged with laboratory methods, but the surface becomes more rough and stiffer. This could be due to the increased asphaltene content and decreased aromatic content or due to the extraction process, which might influence the structural features. A similar surface was acquired by Hofko et. al. [21] for bitumen with an asphaltene content of 30%, suggesting that the asphaltene concentration is responsible for the surface change.

The increase in size in the catana phase correlates with the increase of asphaltene content, as they increase during ageing. The size of the fluorescence centres in the CLSM images stayed relatively constant and they are smaller than the peri-phase and smaller than one direction of the catana phase. Additionally the fluorescence centres appear more spherical than elliptical. An explanation could be the time difference between the conducted measurements. The CLSM images were taken about 4 to 6 hours after sample preparation, whereas the AFM images were taken after a minimum preparation time of 24 hours. There is evidence that the fluorescence centres change between 4 and 24 hours and become more distinct and eventually larger [12]. In addition the ordering process is rather slow and space limited [5,22]. The time for the formation of structural features observed by AFM appears to take up nearly the same amount of time as the occurrence of steric hardening [1,9,10,22,23].

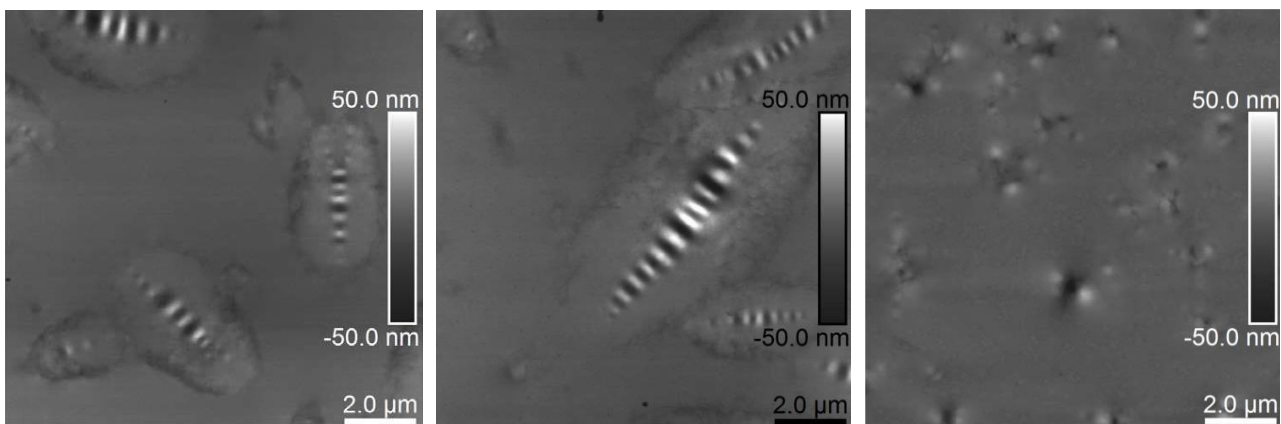


Figure 2: Atomic force microscopy topographical images of 70/100 unaged (left), 70/100 aged (middle) and field sample aged (right)

The “hills” of the catana phase are stiffer than the para-phase and the “valleys” are in the range of the peri-phase. Additionally the peri-phase is surrounded with a small, less stiff boundary layer (Figure 3; brighter colour indicates increasing stiffness). The higher stiffness of the catana phase and peri-phase is likely due to a higher concentration of asphaltenes and resins in these phases. Asphaltenes are known to have a larger contribution to the mechanical properties [1] and with increasing content the samples get stiffer and more brittle [7,21,24]. The layer around the peri-phase is likely to consist of aromatic fractions stabilizing the structures within the para-phase [13].

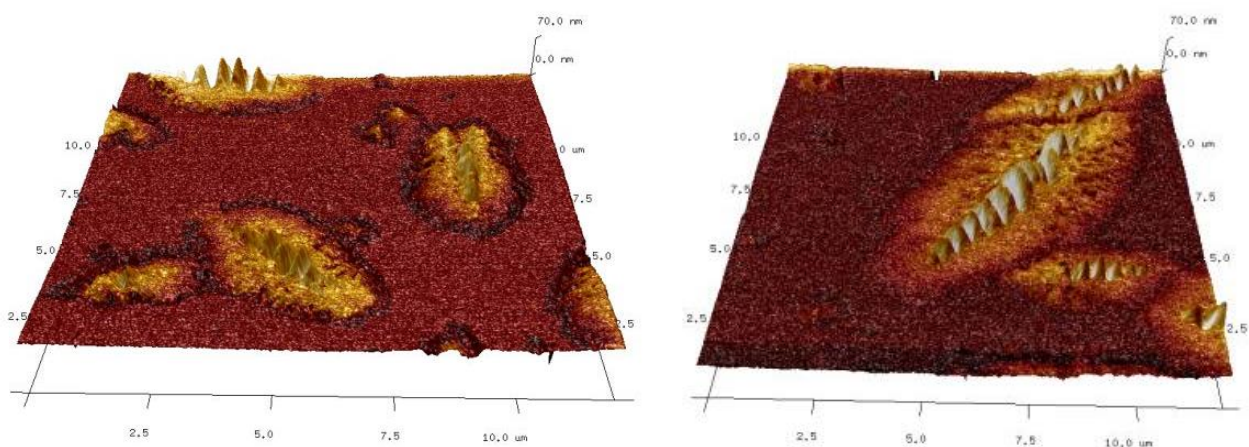


Figure 3: Atomic force microscopy images; overlay of topography and elastic modulus for 70/100 unaged (left) and 70/100 aged (right)

The surface imaged by cryo-transmission electron microscopy is partly due to compression in the direction of the cut (Figure 4). Irregularities in the cutting edge of the diamond knife left string-marks along the cutting direction. The

protuberations are in the range of about 1 μm in length and up to 300 nm in width. The dimension of the features could be bigger, due to the fact that the flakes were not perpendicular to the electron beam. The lack of structural features similar to the surface observed features could indicate that the bulk is more homogeneous and the surface structural features are due to phase separation by surface tension. The centre of the protuberations could consist of smaller agglomerations or crystallisations, due to limited diffusion lengths [5] and contribute towards the recorded image structure. It is also possible, indicated by the size of the flakes, that only the para-phase was investigated and that the stiffer and more brittle encapsulated phases split into tinier pieces during cutting, which were not supported by the grid.

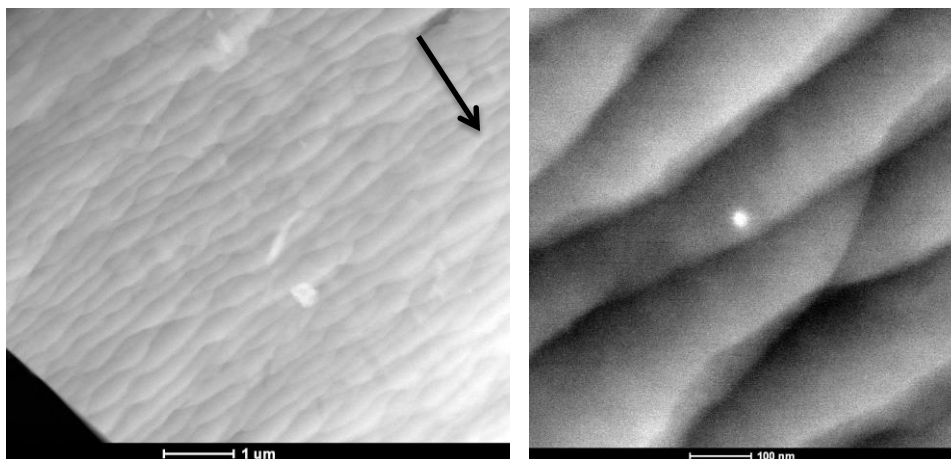


Figure 4: Cryo-transmission electron microscopy images of 70/100 unaged. The arrow in the left figure indicates the cutting direction.

The fluorescence centres of CLSM images and the surface structures of AFM images are time dependent as well as temperature dependent. With increasing temperature the features start to change in size and distribution until at a certain temperature the features vanish and reappear upon cooling [1,10,12]. The time dependency for the structural development is in the same time range as the phenomenon of steric hardening, where molecular restructuring leads over time to harder bitumen. Asphaltenes seems to contribute the most to steric hardening [22]. The investigated features are less to not present in the maltene fraction [11,21], which indicates that asphaltenes are likely to be responsible for the structural formation. But it is still not clear which fraction in fact is responsible for the recorded features, due to observations of similar effects for bitumen waxes. There are two wax types for bitumen: paraffin wax and microcrystalline wax [5, 10]. The amount of these waxes is often determined indirectly by differential scanning calorimeter. The waxes can not be assigned to a defined fraction of the SARA terminology. Saturates and aromatics show a mesophase [22] and are likely to contain wax fractions. *N*-alkanes with chain lengths of about 40 carbons and more become insoluble in *n*-heptane and thus precipitate in the asphaltene fraction [25]. In both cases – asphaltene and wax – a part is extracted from or added to bitumen to visualise the changes in the appearing features. Simulation suggests that long chain paraffin acts as an inducer and the interactions between these fractions could be responsible for the structural features [14]. During ageing primarily the size of the feature increases and to a lesser degree the amount of features, which could be explained due to the lower reactivity of paraffin waxes.

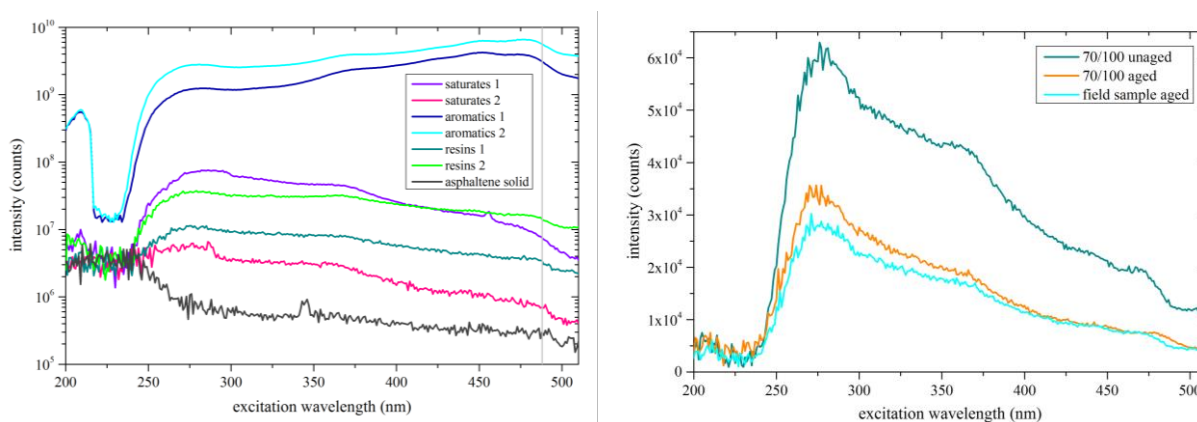


Figure 5: Fluorescence excitation spectra of unaged bitumen fractions (left) and comparison of intensity (right) at 255 nm detection wavelength; the axis of ordinate in the left plot is logarithmical and the grey vertical line represents the excitation wavelength of the CLSM laser

Investigation of the separated fractions with fluorescence spectroscopy revealed that aromatics showed the highest intensity in the region of the detector. Resins and saturates exhibit lesser fluorescence intensity. The signal from asphaltenes in solid state was in the range of the background measurement (Figure 5, left). The fluorescence centres are

therefore likely to contain higher aromatics or have an encapsulation rich in aromatics. Further the intensity decreases with ageing (Figure 5, right), as does the aromatic content. Oxygen is known to quench fluorescence signals. During ageing radicals containing oxygen react with primary aromatics. By taking up oxygen the molecule becomes more polar and shifts toward the classification of asphaltenes. This was confirmed by treating the aromatic fraction with hydrogen peroxide (oxidation agent), which changed the curve of the spectrum and its intensity.

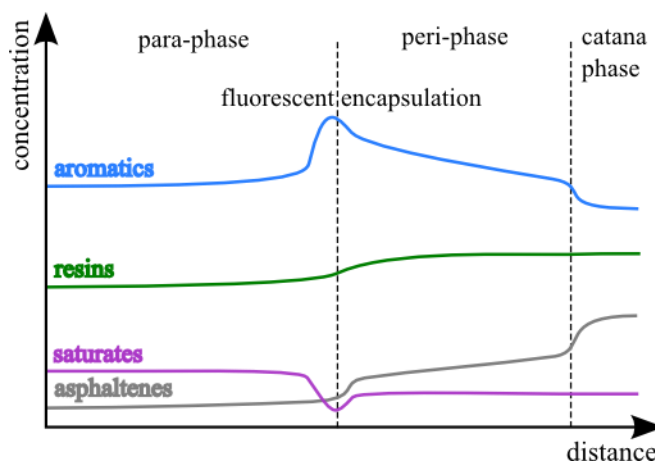


Figure 6: schematic distribution of the SARA fractions within bitumen; allocation of AFM phases and encapsulation responsible for fluorescence

In Figure 6 the lateral sections are used to describe the development of fractional concentration from the matrix towards the centre of a structural feature. The fluorescence centres are allocated to the boundary between the para- and peri-phase, which favours the hypothesis of a fluorescent encapsulation. The aromatic distribution ensures the stability of asphaltenes and resins respectively saturates, due to lesser solubility and insolubility of these fractions into each other, particular between asphaltenes and saturates.

4. SUMMARY AND CONCLUSION

A sample in two different ageing stages – unaged and laboratory aged (PAV) – was investigated with different imaging techniques to find a conclusive connection between the appearing features. CLSM images showed the typical fluorescence centres for both bitumen samples. The sizes of the centres were in both samples in the same range of 1 to 2 μm and a fair connection between the fluorescence centres and the corresponding transmission image exists. Due to the time difference of the image records, the fluorescence centres are smaller in size than the catana respectively peri-phase of the AFM images. The time difference could also be responsible for the same size of the fluorescence centres in both images. The AFM image showed clearly a growth of the catana and peri-phase from unaged to aged bitumen. Responsible for the enlargement is the increase in asphaltene and resin fraction and the nearly constant remaining long chain paraffin waxes, acting as inducer for the structural features. The field aged sample showed that with further increasing of the asphaltene content the structural features change into a rougher surface. TEM images of unaged bitumen showed features of a smaller size compared to the other techniques. The thin cut bitumen flakes had an undulating surface. This could indicate that the bulk is more homogeneous and that the appearing structures are only in the surface region.

ACKNOWLEDGEMENTS

The author thanks Ronald Blab and Hinrich Grothe for initializing the project and the measurements, Florian Handle for helpful discussions; Bernhard Hofko and Markus Hospodka for carrying out the conventional bitumen testing methods and providing the investigated materials; Susanna Neudl for the help at the CLSM. The TEM measurements at USTEM were supported by Johannes Bernardi and Karin Whitmore.

REFERENCES

- [1] The colloidal structure of bitumen: consequences on the rheology and on the mechanism of bitumen modification, Lesueur D., *Advances in Colloid and Interface Science* 42-82, 2009
- [2] Relation between bitumen chemistry and performance, Redelius P., Soenen H., *Fuel* 34-43, 2015
- [3] Identification of four material phases in bitumen by atomic force microscopy, Jäger A., Lackner R., Eisenmenger-Sittner C. Blab R., *Road Materials and Pavement Design* 9-24, 2004
- [4] Low-temperature bitumen stiffness and viscous paraffinic nano- and micro-domains by cryogenic AFM and PDM, Masson J-F., Leblond V., Margeson J., Bundalo-Perc S., *Journal of Microscopy* 191-202, 2007

- [5] On the existence of wax-induced phase separation in bitumen, Schmets A., Kringos N., Pauli T., Redelius P., Scarpas T., *International Journals of Pavement Engineering* 555-563, 2010
- [6] Morphology of asphalts, asphalt fractions and model wax-doped asphalts studied by atomic force microscopy, Pauli A. T., Grimes R. W., Beemer A. G., Turner T. F., Branthaver J. F., *International Journals of Pavement Engineering* 291-309, 2011
- [7] Effect of ageing on the morphology of bitumen by atomic force microscopy, Zhang H. L., Yu J. Y., Feng Z. G., Xue J. H., Wu S. P., *Journal of Microscopy* 11-19, 2011
- [8] Adhesive surface characteristics of bitumen binders investigated by Atomic Force Microscopy, Lyne A. L., Wallqvist V., Birgisson B., *Fuel* 248-256; 2013
- [9] Micromechanical investigation of phase separation in bitumen by combining atomic force microscopy with differential scanning calorimetry results, Das P. K., Kringos N., Wallqvist V., Birgisson B., *Road Materials and Pavement Design* 25-37, 2013
- [10] Surface microstructure of bitumen characterized by atomic force microscopy, Yu X., Burnham N. A., Tao M., *Advances in Colloid and Interface Science* 17-33, 2015
- [11] Direct observation of the asphaltene structure in paving-grade bitumen using confocal laser-scanning microscopy, Bearsley S., Forbes A., Haverkamp R. G., *Journal of Microscopy* 149-155, 2004
- [12] Wax morphology in bitumen, Xiaohu LU, Langton M., Olofsson P., Redelius P., *Journal of Materials Science* 1893-1900, 2005
- [13] The bitumen microstructure: a fluorescent approach, Handle F., Füssl J., Neudl S., Grossegger D., Eberhardsteiner L., Hofko B., Hospodka M., Blab R., Grothe H., *Materials and Structures*, 2014
- [14] Investigating the Interactions of the Saturate, Aromatic, Resin, and Asphaltene Four Fractions in Asphalt Binders by Molecular Simulations, Wang P., Dong Z., Tan Y., Liu Z., *Energy Fuels* 112-131, 2015
- [15] Bitumen and bituminous binders – Determination of the resistance to hardening under the influence of heat and air – Part 1: RTFOT method, European Committee for Standardization, EN 12607-1, 2013
- [16] Bitumen and bituminous binders – Accelerated long-term ageing conditioning by a Pressure Ageing Vessel (PAV), European Committee for Standardization, EN 14769, 2012
- [17] Standard Test Methods for Separation of Asphalt into Four Fractions, ASTM International, ASTM D 4124-01, 2001
- [18] Sensitivity of Asphaltene Properties to Separation Techniques, Alboudwarej H., Beck J., Svrcek W.Y., Yarranton H. W., Akbarzadeh K., *Energy Fuels* 462-469, 2002
- [19] A Review of the Fundamentals of Asphalt Oxidation, Petersen J. C., *Transportation Research Circular E-C140*, 2009
- [20] Relation between bitumen chemistry and performance, Redelius P., Soenen H., *Fuel* 34-43, 2014
- [21] Impact of maltene and asphaltene fraction on mechanical behaviour and microstructure of bitumen, Hofko B., Eberhardsteiner L., Füssl J., Grothe H., Handle F., Hospodka M., Grossegger D., Naha S. N., Schmets A., Scarpas A., *Materials and Structures*, 2015
- [22] Time-Dependent Microstructure of Bitumen and Its Fractions by Modulated Differential Scanning Calorimetry, Masson J-F., Polomark G. M., Collins P., *Energy Fuel* 470-476, 2002
- [23] Steric Hardening and the Ordering of Asphaltenes in Bitumen, Masson J-F., Collins P., Polomark G., *Energy Fuels* 120-122, 2005
- [24] Effects of ageing on the properties of asphalt at the nanoscale, Yuhong Wang P. E., Zhao K., Glover C., Chen L., Wen Y., Chong D., Hu C., *Construction and Building Materials* 244-254, 2015
- [25] Asphaltenes in Bitumen, What They Are and What they Are Not, Redelius P., *Road Materials and Pavement Design* 25-43, 2009